Phycological Research

Phycological Research 2017 doi: 10.1111/pre.12195

Chloroplast position and photosynthetic characteristics in two monostromatic species, *Monostroma angicava* and *Protomonostroma undulatum* (Ulvophyceae), having a shared ecological niche

Jayvee Ablaña Saco,[1] Akio Murakami,[2] Satoko Sekida[1] and Ichiro Mine[1]*

[1]Laboratory of Cell Structure and Function, Graduate School of Kuroshio Science, Kochi University, Kochi, Japan and [2]Kobe University Research Center for Inland Seas, Awaji, Japan

SUMMARY

Monostroma angicava and *Protomonostroma undulatum* are monostromatic green benthic algae (Ulvophyceae), which grow together in the same intertidal habitat of Muroran, Hokkaido, Japan, during the spring season. Commonly, both species have a single chloroplast with one pyrenoid per cell. The parietal chloroplast is located on the periphery of the thallus in both species, although the location of the chloroplast differs in the two. In *M. angicava*, the chloroplast was observed to be arranged on one-side of the thallus surface, whereas, in *P. undulatum*, it was dispersed and randomly located on either side of the thallus or on the lateral face. The density of chlorophylls (Chls) assessed from the absorption spectra of the thallus and its solvent extract was higher in *M. angicava*, which appeared dark-green in color, than in the light-green colored *P. undulatum*. The maximum photosynthetic rate per thallus area (μmol O_2 m^{-2} s^{-1}) was higher in *M. angicava*, whereas, per total chlorophyll content (μmol O_2 g Chl *a* + Chl b^{-1} s^{-1}) was higher in *P. undulatum*. Both species showed similar efficiency of photosynthesis at light-limiting conditions. The efficiency of light absorption by photosystem II (PSII) in *P. undulatum* was higher than *M. angicava*, whereas the photoprotective response was higher in *M. angicava*. This indicates that more energy is utilized in *M. angicava* to protect its PSII due to the chloroplast position, which has more direct exposure to light and, therefore, lowers the efficiency of light absorption by PSII. The higher density of chlorophylls in *M. angicava* could explain higher photosynthesis per thallus area, whereas, higher efficiency of light absorption by PSII in *P. undulatum* could explain higher photosynthesis per total chlorophyll content. The differences in light absorption efficiency and quantum efficiency of PSII might be an important ecological strategy in these two species for their coexistence in the intertidal area.

Key words: chloroplast location, effective quantum yield, initial slope (α), light absorption, maximum photosynthetic rate (*Pmax*), nonphotochemical quenching coefficient (q_N), saturating irradiance.

INTRODUCTION

In Ulvophyceae, the genera *Gayralia, Monostroma, Protomonostroma,* and *Ulvaria* are foliose green algae that are closely related, as inferred from their molecular phylogeny; they are commonly found in marine and estuarine intertidal areas (Bast 2015). They share similar features of gross morphology, having a thallus with a single layer of cells and a single parietal chloroplast per cell, but are distinctly different in their thallus ontogeny and life history (Lobban & Wynne 1981; Brodie *et al*. 2007; Bast 2012). In addition, the shape of the chloroplast among filamentous to tubular genera of Ulvophyceae varies; it is stellate in *Blidingia*, reticulated in *Chaetomorpha*, parietal in *Percusaria*, girdle-shaped in *Ulothrix*, and perforated in *Urospora* and others (Graham & Wilcox 2000; Brodie *et al*. 2007).

In contrast, the position and photosynthetic activity of the single parietal chloroplast in distromatic foliose green algae, *Ulva lactuca var. latissima* (Linnaeus) Decandolle and var. *rigida* (C. Agardh) Le Jolis and *U. mutabilis* Føyn show circadian rhythmic responses. During the daytime, the chloroplast covers the outer face of the cell and exhibits higher photosynthetic activity, whereas during the night, it is along the side walls and shows lowered photosynthetic activity (Britz & Briggs 1976). However, the single parietal chloroplast in distromatic tubular green algae *Enteromorpha intestinalis* (Linnaeus) Link and *E. linza* (Linnaeus) J. Agardh and in monostromatic foliose green alga *Monostroma grevillei* (Thuret) Wittrock is non-motile and always present in the periphery of the thallus surface even when exposed to high light (Britz & Briggs 1976). Because of the simplicity and homogeneity of the thallus and cell morphology among the foliose monostromatic green algae, photosynthetic measurements can be advantageously made through uniform irradiation of the chloroplast from a perpendicular direction. Thus, the relationship between chloroplast morphology and photosynthetic performance could be further elucidated.

Monostroma angicava Kjellman and *Protomonostroma undulatum* (Wittrock) Vinogradova are both monostromatic and benthic green algae that grow in the intertidal areas of Muroran, Hokkaido, Japan. Field observations show that these species coexist on the same rocks and on other seaweeds, like *Gloiopeltis furcata* (Postels & Ruprecht) J. Agardh. They grow abundantly from March to May, and usually disappear by the

**To whom correspondence should be addressed.*
Email: mine@kochi-u.ac.jp
Communicating Editor: Gregory Nishihara
Received 6 January 2017; accepted 5 March 2017.

end of June (Tatewaki 1969). Tatewaki (1969) observed the differences in the development of their fronds; *M. angicava* was observed to give-off erect saccate fronds that develop into the expanded monostromatic membrane, whereas, the erect filaments of *P. undulatum* directly developed into the expanded monostromatic membrane.

Moreover, the surface view of both the species captured in the micrographs of Tatewaki (1969) revealed a degree of variation in their appearance. In *M. angicava*, the cells appeared to have a single parietal chloroplast localized uniformly along the thallus surface (plate IX, figs D, E in Tatewaki 1969), whereas the cells of *P. undulatum* had a single chloroplast and seemed to have an uneven appearance and its position seemed to be different among the cells (plate IV, fig. D in Tatewaki 1969). This indicates the possibility that the intracellular chloroplast localization is different between the two species.

In addition, Hori (1973) observed a more complex ultrastructure of the pyrenoid in *M. angicava* showing matrix material divided into 6–12 compartments by the intrusion of many interpyrenoidal bands of a single thylakoid, than in *P. undulatum* that showed six compartments lacking thylakoid elements within the matrix. The same author mentioned that it would be interesting to correlate these differences with their metabolic function in photosynthesis. Because the two closely-related species that coexist on the same habitat are distinct in their chloroplast distribution pattern, these two species might also have distinct photosynthetic characteristics that might provide insights on their coexistence in the intertidal area. We examined the relationship between the chloroplast location and the photosynthetic performance by microscopic observations of the chloroplast location from the surface and in sectional views and determined the content of photosynthetic pigments as well as the various parameters of photosynthesis.

MATERIALS AND METHODS

Algal material

M. angicava and *P. undulatum* were collected from the intertidal area of Botofurinai, Muroran, Hokkaido, Japan (42°18′20″N, 140°59′02″E) from 29 April to 5 May 2016, at low tide (Fig. 1a,b). The thalli of *M. angicava* appeared dark green and sturdy, whereas those of *P. undulatum* appeared light green and fragile (Fig. 1c,d). The samples were transported to the laboratory within 30 min of collection and the debris, epiphytes, and epizoans present on the surface of thalli were cleaned off. Until further processing, these thalli were maintained in an outdoor plastic container filled with natural seawater. A different set of individual thallus was used in each experiment.

Microscopic observation of the shape and location of chloroplasts

Cellular morphology and the location of the chloroplast were observed in the surface view and in the thin cross-sections of the intact thalli without fixation. Some thallus sections

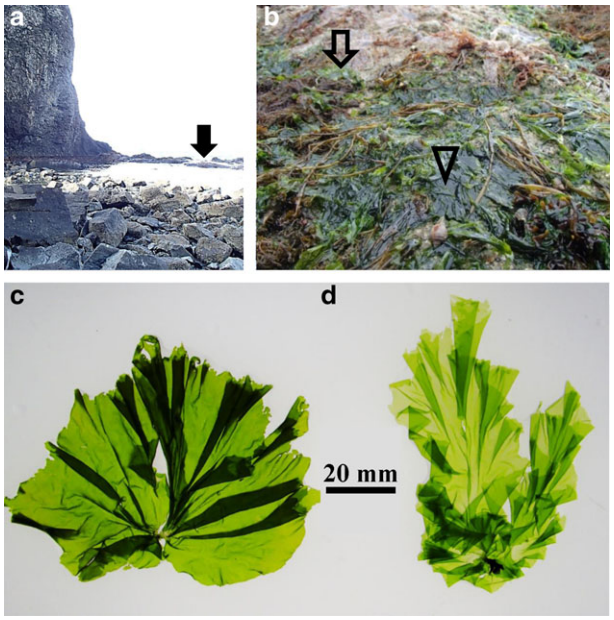

Fig. 1. Photographs of the collection site (a, b) and freshly collected samples (c, d) of *Monostroma angicava* and *Protomonostroma undulatum*. (a) Intertidal area where the samples were habituated (filled arrow). (b) Closer image of two species co-habituated on the rock. Empty arrowhead and arrow indicate *M. angicava* and *P. undulatum*, respectively. (c) *M. angicava* showing dark green-colored and sturdy thallus having segmented, fan-shaped blade, with a plane or lobed margin. (d) *P. undulatum* showing light green-colored and fragile thallus having a lanceolate blade with prominent wrinkled or ruffled margin.

including the young saccate thalli of *M. angicava* were chemically fixed with 1% glutaraldehyde at room temperature for 30 min. The fixed thallus sections were washed with filtered seawater and the nuclear DNA was stained with 0.01 mg mL^{-1} SYTO-13 (Life Technologies Japan Ltd., Yokohama, Japan) at room temperature for 30 min. The fixed saccate thalli were dehydrated with ethanol, and were infiltrated and embedded with butyl-methyl methacrylate (Gubler 1989). Two micrometer-thick sections perpendicular to the long axis of the saccate thalli were cut with a glass knife using an ultramicrotome (UCT, Leica Microsystems, Wetzlar, Germany); the sections were collected on a glass slide and stained with Toluidine Blue O (Waldeck GmbH & Co. KG, Münster, Germany). The observations were made using an Olympus BX50W light microscope and the microphotographs were taken by a Zeiss AxioCam Hrc digital camera. ImageJ 1.49 version computer software (Rasband 2016) was used to measure the microscopic dimensions of the cells.

Absorption spectra of the intact thalli and extracts of photosynthetic pigments

Photosynthetic pigments were analyzed using the absorption spectra of intact thalli and the solvent extract of thalli determined with a double-beam spectrophotometer (JASCO UV–VIS V-550, JASCO Corporation, Tokyo, Japan). For the measurement of the absorption spectra of photosynthetic pigments

in intact thalli, the opal-glass transmission method for turbid and scattered samples was applied to remove the effect of light scattering by the thallus (Shibata 1959). One layer of thallus sample was held between two cover slide glasses and put in the sample cuvette. Three sheets of paraffin paper were substituted for the standard opal-glass. Absorption spectra were normalized to zero at 750 nm.

The contents of chlorophyll (Chl) *a* and Chl *b* were measured after extraction with 1.0 mL 100% N, N-dimethylformamide (DMF) from thallus samples (ø = 8 mm) at room temperature in the dark for 1 h. The extracted solutions were used for the measurement of the absorption spectra. The absorbance of the extract with a light path of 10 mm was measured by the same spectrophotometer as mentioned above. The concentration of chlorophylls was calculated according to Porra *et al*. (1989) following the equation [Chl *a* + Chl *b* (μg ml^{-1}) = 17.67 $A_{646.8}$ + 7.12 $A_{663.8}$].

Measurement of photosynthetic oxygen evolution

The photosynthetic oxygen evolution of a thallus disc of 8-mm in diameter (n = 5) was measured with a Clark-type oxygen electrode (9002SP, Toko Chemical Laboratories Co., Ltd., Tokyo, Japan) and a glass specimen chamber (OC-100, Toko Chemical) at 10 ± 2 and 15 ± 2°C controlled by a recirculating water jacket connected to a water bath. These were placed inside a sealed black box to prevent ambient light intrusion and for the measurement of the respiratory oxygen uptake rate. The discs were punched about 12 h in advance and kept in an outdoor culture dish filled with filtered seawater to heal wounding.

The water bath was made from a copper plate and placed in the middle of a large Styrofoam container where ice packs and ice were placed on both sides to achieved the desired temperature and monitored by laboratory thermometer inserted in the water bath. The temperature used were the surface water temperature of about 10°C during sample collection (Muroran Marine Station 2016).

The light was provided by a halogen lamp (JDR110V60W/K5S, Toshiba Lighting and Technology Corp., Yokosuka, Japan) and two heat-absorbing filters (HA-50, Hoya Corporation USA, Milpitas, USA), from the bottom of the specimen chamber using a light guide. The light intensity was attenuated by neutral density filters (AND-25S-01, 05, 13, 25, 50, 70, Sigma Koki Co., Ltd., Tokyo, Japan) and measured with a phototransistor (NJL7502L, New Japan Radio Co., Ltd., Tokyo, Japan) housed in a black painted aluminum tube inserted into the chamber, calibrated with a quantum meter (BQM, Apogee Instrument, Inc., Logan, USA).

The disc was placed on the raised bottom of the specimen chamber filled with 0.6 mL filtered seawater and a round piece cut from a stainless steel mesh (PMY40X-K-50-50, Misumi Corporation, Tokyo, Japan) was placed on top of the thallus disc to immobilize it during continuous stirring by a cylindrical magnetic stirrer placed on top. The bottom was raised about 9 mm to minimize the inner capacity by placing a transparent acrylic column with an outer diameter exactly fitted to the inner diameter of the cylindrical chamber. The disc was subjected to eight progressively increasing light intensities. Photosynthetic oxygen evolution rate was traced for 3 min before which the light was turned off for 3 min to trace the respiratory oxygen uptake rate, replacing the filtered seawater before each cycle.

The current signal of the oxygen electrode was converted to a voltage signal and amplified by Hansatech oxygen control box (CB1-D3, Hansatech Instrument, Ltd., King's Lynn, England). The oxygen electrode was calibrated according to an oxygen solubility table (YSI Incorporated 2009) at salinity 36.1 ppt and atmospheric pressure 760 mmHg, at the saturated level and at oxygen-depleted level using 2% Na_2SO_3 in 10 mM $Na_2B_4O_7$ solution to their respective temperature. The photosynthetic and respiration rates were calculated from the slope of the dissolved oxygen within the 3-min incubation time.

PAM fluorometry

The chlorophyll fluorescence of a thallus disc of 8-mm in diameter (n = 5) was measured with a PAM fluorometer (JUNIOR-PAM Chlorophyll Fluorometer, Walz, Effeltrich, Germany) using 0.6 μmol photons m^{-2} s^{-1} measuring light and 6000 μmol photons m^{-2} s^{-1} saturating pulse at 10 ± 2 and 15 ± 2°C. The discs were punched about 12 h in advance and kept in an outdoor culture dish filled with filtered seawater to heal wounding. The disc was immobilized in a specimen holder at a distance approximately 1 mm from the light fiber optics, which was inserted in a tin container filled with filtered seawater under continuous stirring and placed inside a deep container with recirculating water jacket connected to a water bath as described above.

An example of the PAM fluorescence measurements divided into dark and light adapted states is shown in Fig. S1 of the Supporting Information. The disc was dark adapted for 10 min before giving a saturating pulse for measurement of the maximum quantum yield of PSII [$F_V/F_M = (F_M - F_O)/F_M$] (Genty *et al*. 1989). Thereafter, the disc was light adapted under a saturating actinic light (820 μmol photons m^{-2} s^{-1}) reaching stable fluorescence about 20 min before providing the saturating pulse to measure the efficiency of light absorption by PSII or effective quantum yield of PSII [$\phi_{PSII} = (F_M' - F')/F_M'$] (Genty *et al*. 1989). The far-red light was given at the end of light adapted measurement to determine the nonphotochemical quenching coefficient [$q_N = 1 - [(F_M' - F_O')/(F_M - F_O)]$] (van Kooten & Snel 1990). The stable fluorescence denotes an almost constant level of fluorescence after a sufficiently long actinic light illumination that was achieved within 2–5 min. Thereafter, 3–5 saturating pulses were given at every 5–10 s, producing 3–5 ϕ_{PSII} values that were averaged to represent the ϕ_{PSII} at saturating actinic light.

Data analysis

The photosynthetic rates at eight different light intensities were curve-fitted using a non-linear least square regression comparing differences between measured and calculated values with Solver Module in Excel (Microsoft Corp., Redmond, USA) (Roleda *et al*. 2006), following a model using an exponential equation (Webb *et al*. 1974; Jassby & Platt 1976; Platt *et al*. 1980; Henley 1993) as cited by Borlongan *et al*. (2017) [$P^n = Pmax((1 - exp(-\alpha/Pmax)(I)) - Rd$], where, P^n is the net photosynthesis, $Pmax$ is the maximum

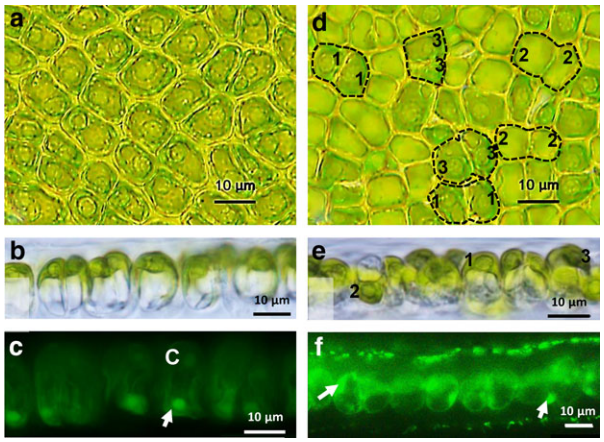

Fig. 2. Light microphotographs of the vegetative thallus of *M. angicava* (a–c) and *P. undulatum* (d–f). (a, d) Intact surface views, (b, e) Intact cross-sectional views, (c, f) Cross-sectional views of chemically-fixed specimens stained with SYTO-13 where the position of chloroplast (C) and green fluorescent nuclei (arrows) are indicated. In (d), some pairs of two closely positioned cells, probably derivative of cells from the latest cell division, are encircled by broken lines and the types of chloroplast localizations are indicated by a number, i.e., (1) surface localized at one-side, (2) surface localized at the other side, and (3) lateral face side. Note that the small green fluorescent dots in the upper/lower sides in (f) are derived from the adhesive bacteria along the thallus surfaces stained by SYTO-13.

photosynthesis, α is the initial slope of the curve, *I* is the incident irradiance and *Rd* is the dark respiration. The saturation and compensation irradiance were computed as *Ik* (=*Pmax*/α) and *Ic* [=*Pmax*(*ln*((*Pmax*)/(*Rd* – *Pmax*))/α], respectively. The procedure of Dawes (1992) was used to allow statistical comparison of the *P-I* curve parameters where respective photosynthetic rate per light level from each disc of five different individuals was curve-fitted producing five data for each parameter.

One-way analysis of variance (ANOVA) was used to determine significant differences in the *P-I* curve and PAM fluorescence parameters between the two species to each temperature ($P < 0.05$) after subjecting the data to normality test using Shapiro–Wilk, or the data, i.e., α and *Ik*, was log transformed if it was not uniformly distributed. Regression analysis was also done to determine the relationship among *P-I* curve parameters on each species to temperature. These were done using R software (version 3.2.0, R Core Team, Vienna, Austria).

RESULTS

Cell and chloroplast morphology

The two monostromatic green benthic algae, *M. angicava* and *P. undulatum*, are closely related species and share an ecological niche (Fig. 1). However, the microscopic observations of the thalli showed differences in the cell morphology and the intracellular position of chloroplasts between the two species (Fig. 2). The cellular and chloroplast dimensions in the two species are summarized in Table 1.

The surface view of the thalli revealed that the shapes of cells were distorted polygonal or rectangular in both the species. The cell size of *M. angicava* was larger (×1.2 in the surface view and ×1.8 in the cross-sectional view) than that of *P. undulatum* (Fig. 2a,b,d,e). The cell density of *P. undulatum* was slightly higher than that of *M. angicava* measured from the number of the cells in the microphotographs in surface view within 50 µm^2.

The cells of both the species have a single chloroplast in common, with a single pyrenoid, located peripherally along the inside of the cell wall (i.e., in the parietal location). The chloroplast of *M. angicava* was uniformly arranged on one side of thallus surface of the monostromatic thallus (Fig. 2b). This biased unilateral arrangement seemed to be unchanged from the early developmental stage, where the chloroplast in each cell was uniformly positioned along the outer surface of the saccate thallus (Fig. 3). In contrast to this arrangement, the chloroplasts of *P. undulatum* were located in various positions on either surface or on the face lateral to the neighboring cells of the monostromatic thallus (Fig. 2e). The arrangement of chloroplast in *P. undulatum* was conveniently classified into three positions: surface localized at one-side (P1), surface localized at the other side (P2), and localized on the lateral face (P3) (Fig. 2d). The same positioning of the chloroplasts was observed in most of the paired neighboring cells, probably derived from the common mother cell after the latest cell division (Fig. 2d, broken lines). The intracellular position of the nucleus was on the other side of the chloroplast in both the species (Fig. 2c,f).

Composition of photosynthetic pigment and capacity of light absorption in thallus

To compare the photosynthetic properties of both the monostromatic species with different chloroplast arrangement, the property of light absorption and the composition of photosynthetic pigments was determined (Fig. 4, Table 2).

The *in vivo* absorption spectra of the intact thalli (measurements from a single layer) had almost a similar spectral shape but were remarkably different in their magnitudes in the two species where *M. angicava* had a higher absorption spectra than *P. undulatum* (Fig. 4a). Similarly, the absorption spectra of DMF-extracted solutions was higher in the dark-green thallus of *M. angicava* with 3.4-times higher content of Chl *a* and Chl *b* than in the light-green thallus of *P. undulatum* (Fig. 4b, Table 2). Both species showed similar values in the ratio of Chl *a* to Chl *b*.

Absorption spectra of the red wavelength region were used in comparing the light absorption capacity of the thallus between *M. angicava* and *P. undulatum*. The ratios of the absorption maxima at 679 nm (A_{679}) of the intact thalli and at 664 nm (A_{664}) of the extracted chlorophyll were 0.46:0.13 (=3.5) and 0.34:0.10 (=3.4), respectively. The fold difference was nearly equal (3.4–3.5), which might indicate that the light absorption capacity of the thalli of both species was dependent on the total chlorophyll content.

Table 1. Cellular and chloroplast morphology of *Monostroma angicava* and *Protomonostroma undulatum*

Species	Cellular dimension (μm)		Cell density (cells/μm^2)	Chloroplast dimension (μm)		Chloroplast localization
	Surface view	Sectional view		Main body	Lobes	
M. angicava	9–15 × 6–13	19–21	ca. 26	5–6 × 9–12	3–4	Uniform[†]
P. undulatum	8–12 × 6–9	11–13	ca. 35	4–6 × 8–10		Various[‡]

[†]A single parietal chloroplast is located along the surface of the same side of thallus in all the cells.
[‡]A single parietal chloroplast is located along the surface of either side of the thallus or along the side wall, varying in each cell.

Activity of the photosynthetic oxygen evolution

We compared the photosynthetic activity to the irradiance (*P-I*) curve per thallus area (μmol O_2 m^{-2} s^{-1}) and per the Chl *a* and Chl *b* content (μmol O_2 g Chl *a* + Chl b^{-1} s^{-1}) in the two species (Fig. 5; Tables 3–4).

The maximum photosynthetic oxygen evolution rate at the light-saturated level (*Pmax*) was remarkably different between the two species (Fig. 5). The value of *Pmax* per thallus area was higher in *M. angicava* than in *P. undulatum* (Fig. 5a,b) whereas the *Pmax* per total chlorophyll content was higher in *P. undulatum* than in *M. angicava* (Fig. 5c,d). *Pmax* seems to be temperature dependent ($P < 0.01$). The respiration rate per thallus area and per total chlorophyll content did not differ significantly between the species at either temperature. Generally, α did not differ in both the species at either temperature. *Ik* was lower at 10°C and higher at 15°C in both the species and seems to be temperature dependent ($P < 0.05$) while *Ic* did not differ significantly between the species at either temperature.

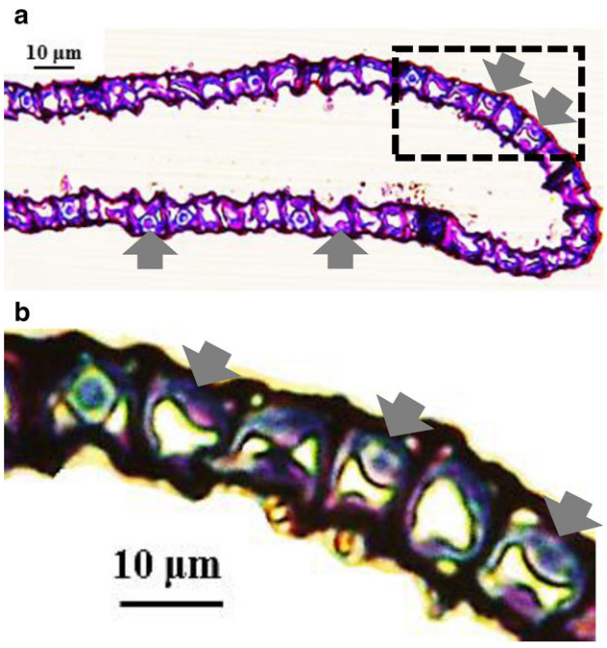

Fig. 3. Light microphotographs of the embedded young saccate thallus of *M. angicava* in cross-sectional view at lower magnification (a) showing uniformly located chloroplast (gray arrow) on the periphery of the thallus surface on the outside of the saccate thallus and at a higher magnification (b) shown in the dashed box in (a).

PAM fluorometry

We characterized the three parameters, F_V/F_M, ϕ_{PSII}, and q_N by measuring the PAM fluorescence in the two species (Fig. 6).

In the dark-adapted state, the F_V/F_M had almost the same value between the two species at either temperature. In the light-adapted state, the value of ϕ_{PSII} was significantly higher in *P. undulatum* than in *M. angicava* at either temperature. The value of q_N was significantly higher in *M. angicava* than in *P. undulatum* at either temperature.

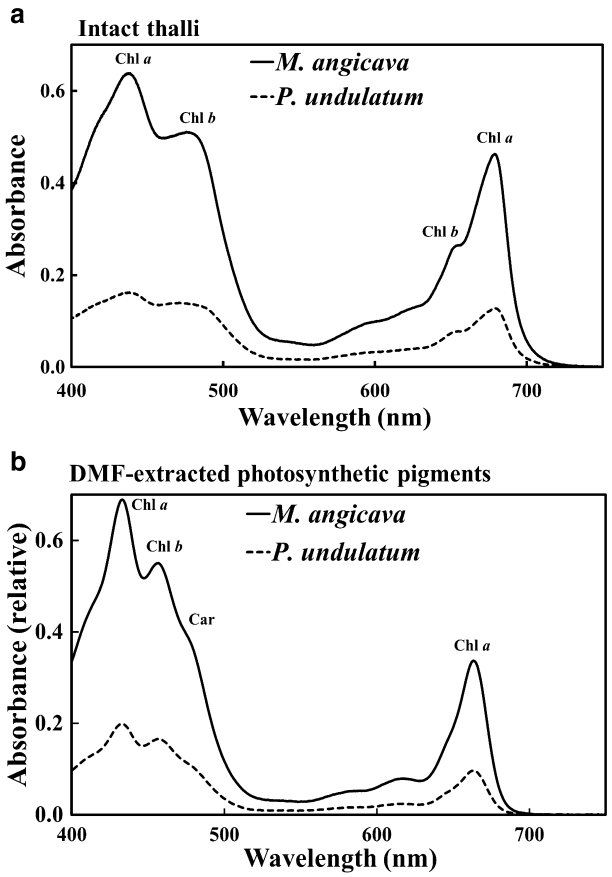

Fig. 4. Absorption spectra of the intact thalli (a) and DMF-extracted photosynthetic pigments (b) of the two monostromatic green algal species (Chl *a*: chlorophyll *a*, Chl *b*: chlorophyll *b*, car: carotenoids). See the text for further details.

Table 2. Light absorbance of the thallus and chlorophyll content of *M. angicava* and *P. undulatum* (data from five different individuals are shown)

Species	Thallus absorbance ($\Delta A_{679-750}$)	Chlorophyll content (μg Chl *a* + Chl *b*/cm^2 thallus area)	Chl *a*/Chl *b* ratio (mol/mol)
M. angicava	0.46 ± 0.06	5.33 ± 0.57	1.98 ± 0.04
P. undulatum	0.13 ± 0.02	1.56 ± 0.09	1.78 ± 0.13

DISCUSSION

The present study of these two closely related monostromatic species showed differences in the chloroplast position and photosynthetic performance. In *M. angicava*, the chloroplast position was uniformly distributed along the periphery of the thallus surface. The higher light absorption in both thallus and extracted chlorophyll in *M. angicava* could explain higher *Pmax* per thallus area. In *P. undulatum*, the chloroplast position was variously located among cells which on the either side of the thallus surface or on the face lateral to the neighboring cells. The higher ϕ_{PSII} in *P. undulatum* could explain higher *Pmax* per total chlorophyll content. Moreover, the higher q_N in *M. angicava* shows a higher photoprotective response in the protection of PSII due to the chloroplast position which has more direct exposure to light thus lowering $\phi_{PSII.}$

Cellular morphology and intracellular position of chloroplasts

Among the monostromatic green algae (Monostromataceae), reports describing the morphology and location of chloroplasts in *P. undulatum* are few; these include the original description of the species by Vinogradova (1969). The genus *Monostroma* has been well-described and has a single, parietal chloroplast with a single pyrenoid (van den Hoek *et al*. 1995;

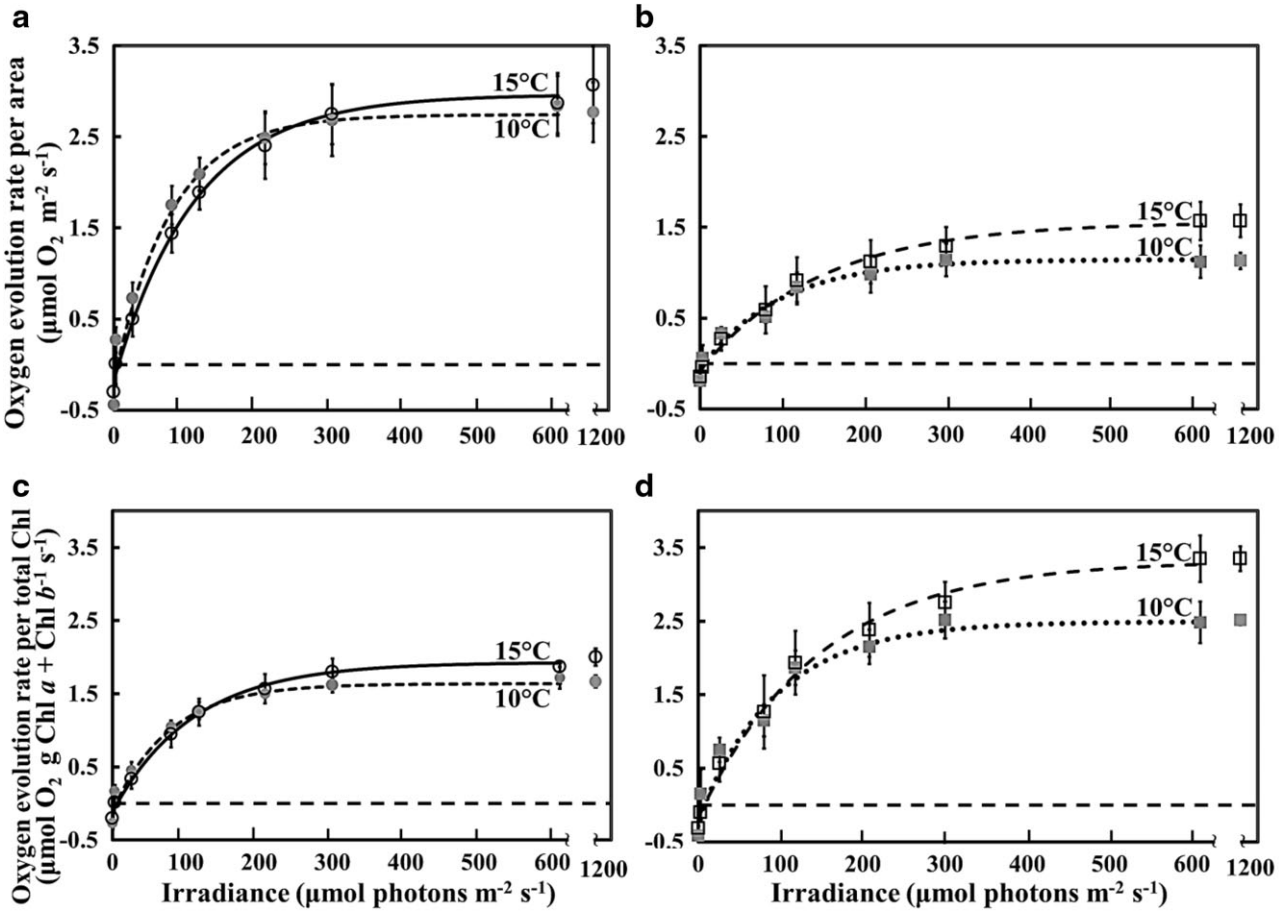

Fig. 5. Photosynthesis-irradiance (*P-I*) curve of *M. angicava* (a, c) and *P. undulatum* (b, d). (a, b) per thallus area and (c, d) per total chlorophyll content. The photosynthetic rate was curve-fitted up to the highest irradiance level but the line regression after 600 μmol photons m^{-2} s^{-1} was omitted to show the photosynthetic rates at lower irradiance level. Marker and vertical line are a mean and standard deviation from discs of five different individuals, respectively. See the text for further details.

Table 3. *P-I* curve parameters of *M. angicava* and *P. undulatum* at different temperatures

Species	Temperature (°C)	Parameters of photosynthesis-irradiance (*P-I*) curve							
		per thallus area†			per total chlorophyll content‡			*Ik*§	*Ic*§
		Pmax	*Rd*	*α*	*Pmax*	*Rd*	*α*		
M. angicava	10	2.92 ± 0.32 a	0.06 ± 0.01	0.04 ± 0.00 a	1.76 ± 0.05 a	0.06 ± 0.02	0.02 ± 0.00	78 ± 14	2.62 ± 0.48
P. undulatum		1.21 ± 0.21 b	0.05 ± 0.05	0.01 ± 0.00 b	2.68 ± 0.33 b	0.07 ± 0.05	0.03 ± 0.01	94 ± 18	2.25 ± 1.37
M. angicava	15	3.17 ± 0.53 a	0.06 ± 0.04	0.03 ± 0.01 a	2.05 ± 0.17 a	0.06 ± 0.06	0.02 ± 0.00	113 ± 33	3.31 ± 2.45
P. undulatum		1.65 ± 0.14 b	0.05 ± 0.03	0.01 ± 0.00 b	3.56 ± 0.07 b	0.06 ± 0.03	0.02 ± 0.01	156 ± 50	2.49 ± 1.56

†μmol O_2 m^{-2} s^{-1}.
‡μmol O_2 g Chl *a* + Chl *b*$^{-1}$ s^{-1}.
§μmol photons m^{-2} s^{-1}.
ANOVA at $P < 0.05$, mean ± standard deviation with the same letter is not significantly different; data from discs of five different individuals are shown.

Graham & Wilcox 2000; Brodie *et al*. 2007), specifically in *M. grevillei* (Bliding 1968) or it has a single and parietal, cup-shaped chloroplast with a single pyrenoid as in *M. oxyspermum* (Kützing) Doty (Gayral 1965). In contrast, cells of the other genus *Gayralia* and *Ulvaria* of Monostromataceae have a parietal chloroplast with one or many pyrenoids (Brodie *et al*. 2007; Pellizzari *et al*. 2013). Moreover, the chloroplasts in *M. grevellei* are non-motile and were always seen in the periphery of the thallus surface even under high light intensity (Britz & Briggs 1976), and we did not observe any signs of chloroplast movement in *M. angicava* and *P. undulatum* during our microscopic observation throughout all experiments of the present study.

The location of nucleus opposite to that of the chloroplast in both the species, as observed in this study, was in contrast to the observation of Løvlie and Bråten (1970) on the distromatic *Ulva mutabilis* showing that the nucleus is located between the parietal chloroplast and the inner cell wall positioned-vacuole. However, the *Monostroma nitidum* Wittrock collected from Kochi, Japan showed a similar location of nucleus as in *U. mutabilis* (Jayvee Ablaña Saco *et al*. unpubl. data, 2015).

This study further described the morphology and location of chloroplast in *P. undulatum*, which has a single, parietal chloroplast with a single pyrenoid along the periphery of the thallus surface. The chloroplast was observed to be located differently in different cells; it was either surface localized on one-side, surface localized on the other-side, or was localized on the lateral face. Okazaki *et al*. (2010) discussed that the parental chloroplast in algae divides in synchrony with the division of the host eukaryotic cell. This is mediated by both the chloroplast and host-nucleus division genes; however, the chloroplast gene expression is mainly regulated by the host cell division cycle. This indicates the possibility that the inherited chloroplast localization in the cells derived from their parent cells could be regulated and facilitated by the host eukaryotic cell. Further detailed investigations on cell division would be necessary to understand the mechanisms underlying the inheritance of the chloroplast location in the derivative cells of *P. undulatum*.

General photosynthetic features of *M. angicava* and *P. undulatum*

The same *α*, *Ic*, and *Ik* obtained from *M. angicava* and *P. undulatum* were within the range of other intertidal green benthic algae i.e., *Caulerpa paspaloides* (Bory) Greville (*α*: 0.02–0.05; *Ic*: 1–13 μmol photons m^{-2} s^{-1}; *Ik*: 38–111 μmol photons m^{-2} s^{-1}; O'Neal & Prince 1988); *C. prolifera* (Forsskål) Lamouroux (*α*: 0.02–0.31; *Ic*: 3–21 μmol photons m^{-2} s^{-1}; *Ik*: 11–112 μmol photons m^{-2} s^{-1}; Terrados & Ros 1992); *Chaetomorpha linum* (Müller) Kützing, *Enteromorpha intestinalis, Ulva lobata* (Kützing) Harvey, and *U. rigida* C. Agardh (*α*: 0.04–0.13; *Ic*: 6–11 μmol photons m^{-2} s^{-1}; *Ik*: 50–82 μmol photons m^{-2} s^{-1}; Arnold & Murray 1980). The same *α* and *Ic* in *M. angicava* and *P. undulatum* could reflect similar efficiency and capacity on photosynthesizing under low light regimes, similarly to the observation of O'Neal and Prince (1988) and Terrados and Ros (1992) on the green benthic algae, *C. paspaloides* and

Table 4. Regression coefficient (r^2) of the *P-I* curve parameters to temperature in *M. angicava* and *P. undulatum*

Species	Parameters of photosynthesis-irradiance (*P-I*) curve							
	per thallus area†			per total chlorophyll content‡			*Ik*§	*Ic*§
	Pmax	*Rd*	α	*Pmax*	*Rd*	α		
M. angicava	0.08	0.02	0.34	0.62**	0.00	0.28	0.44*	0.04
P. undulatum	0.62**	0.00	0.16	0.79**	0.03	0.09	0.53*	0.01

$^{**}P < 0.01$, $^{*}P < 0.05$.
†μmol O_2 m^{-2} s^{-1}.
‡μmol O_2 g chl $a + b^{-1}$ s^{-1}.
§μmol photons m^{-2} s^{-1}.
Data from discs of five different individuals are shown.

C. prolifera, respectively, having steeper α and low *Ic* during the winter season which is characterized by low light availability.

The *Ik* seems to be dependent on temperature on both *M. angicava* and *P. undulatum* that could reflect an adaptation to optimize photosynthesis to low and high light conditions, similarly to the observation of Xiao *et al*. (2016) in the green benthic alga, *U. prolifera* Müller showing increasing saturating irradiance with temperature indicating tolerance to high irradiance. Moreover, no decrease in photosynthesis and no photoinhibitory responses were observed beyond the saturating irradiance for both *M. angicava* and *P. undulatum*, which was similar to observations in Maegawa and Aruga (1974) and Xiao *et al*. (2016) in the green benthic algae, *Monostroma latissimum* Wittrock and *U. prolifera*, respectively, and indicate tolerance to high irradiance. Watanabe *et al*. (2014) also found no photoinhibitory responses in the monostromatic red alga, *Pyropia tenera* (Kjellman) Kikuchi *et al*. (= *Porphyra tenera* Kjellman), which were collected from a mariculture site at the seawater surface.

The high α and low *Ic* obtained from both *M. angicava* and *P. undulatum* could also reflect the period these species grow dominantly, i.e., March to May, under shorter photoperiod and low solar irradiation. Ichiki *et al*. (2001) characterized the winter and early spring in southwestern Hokkaido as severely limited in irradiance. Moreover, the *Ik* was high and *Pmax* was kept high even under the strongest light used in the present study (1211 μmol photons m^{-2} s^{-1}) in both *M. angicava* and *P. undulatum*. This could also reflect that the higher intertidal zone where they are growing is regularly exposed to strong irradiation during tidal emersion.

The majority of the temperate green benthic algae showed an increase in photosynthesis with increasing temperature and subsequent decreases, thereafter, to a certain extent (Terrados & Ros 1992; Zou & Gao 2014; Xiao *et al*. 2016). This could reflect short-term response on the capacity in adapting to increasing temperature. We could only assume that the dependence of *Pmax* to temperature of both *M. angicava* and *P. undulatum* was due to a limited temperature of 10 and 15°C used in this study.

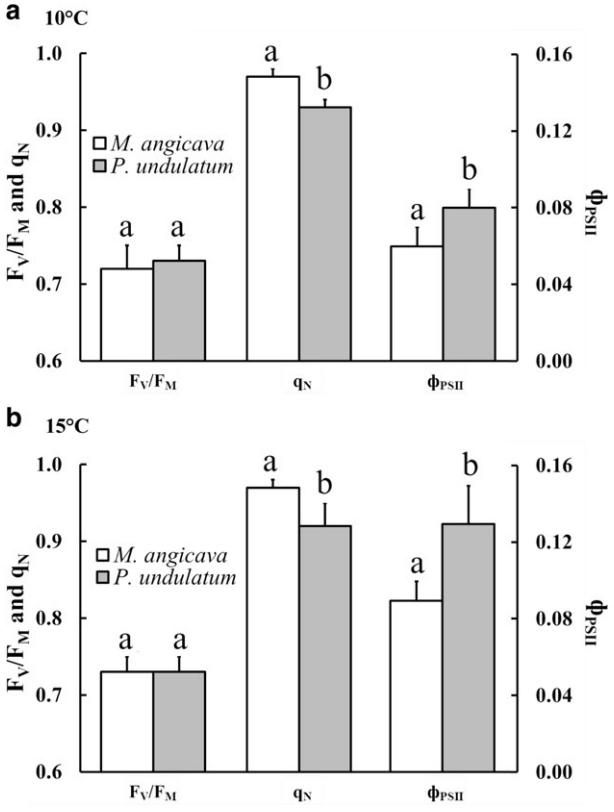

Fig. 6. PAM fluorescence parameters of two monostromatic seaweed species at 10°C (a) and 15°C (b). Vertical bars with the same letter are not significantly different. Vertical bar and vertical line are a mean and standard deviation from discs of five different individuals, respectively. See the text for further details.

Photosynthesis and light absorption by chlorophylls

As estimated by *Pmax* per total chlorophyll content, the photosynthetic performance of *P. undulatum* was 1.5- and 1.7-fold higher than that of *M. angicava* at 10 and 15°C, respectively. This difference could possibly be attributed to the following causes: (i) higher efficiency of light absorption by chlorophyll in *P. undulatum* and (ii) higher effective quantum efficiency of PSII in *P. undulatum*. However, the absorption spectra of the thallus and the extracted chlorophyll were higher in *M. angicava* than that of *P. undulatum*, reflecting the different densities of photosynthetic pigments per thallus area. This indicates that the thallus of *M. angicava* has higher

light absorption capacity for photosynthesis than that of *P. undulatum*. Frost-Christensen and Sand-Jensen (1992) observed that on the basis of thallus area, the photosynthetic efficiency in *Ulva lactuca* Linnaeus increased with the increasing absorption and pigmentation; for example, thallus with a 2.7-fold difference in photosynthetic efficiency (mol O_2 mol^{-1} incident photons), had a 2.3-fold difference in the percent absorption (%) and 4.5-fold difference in the chlorophyll density (mg m^{-2}). Although both species had a similar ratio of Chl *a* to Chl *b*, indicating similar sizes of the light-harvesting antenna pigments, higher light absorption capacity was observed in *M. angicava* compared to *P. undulatum*.

The lower ratio between the maximum absorbance of thallus and content of extracted chlorophylls in both *M. angicava* and *P. undulatum* might indicate that light absorption efficiency of the thallus was primarily due to the efficiency of chlorophyll content in the harvesting of light. Ramus (1990) showed a direct correlation between the pigment content and *P-I* responses which are likely restricted to species with thin homogeneous tissues, i.e., monostromatic and distromatic species, in which all cells contain chlorophyll rich organelle—chloroplast. In addition, the photon gradient is not possibly existing with thin homogeneous tissues, showing that photosynthesis is proportional to the absorbance per unit pigment content. Although a 1.3-fold higher cell density was observed in *P. undulatum* than in *M. angicava*, the latter species might have an advantage because of the uniformly-located chloroplast on the periphery of the thallus surface, which could have a more direct exposure to light, thereby, increasing the light absorption efficiency than in the chloroplasts with varied locations in the former species.

Photosynthetic characteristics revealed by chlorophyll fluorescence

To examine the other possible reason for the difference in photosynthetic capacity between the two species, we measured ϕ_{PSII} and observed 1.3- and 1.4-fold higher values in *P. undulatum* than those in *M. angicava* at 10 and 15°C, respectively. This suggests that the difference in the photosynthetic capacity could partially be attributed to the difference in ϕ_{PSII}. Lin *et al*. (2011) showed higher ϕ_{PSII} in the light-green floating thalli with a single chloroplast located on the edge of the cell in surface view and having lower chlorophyll content than in the dark-green thalli with chloroplast occupying over the whole cell area and having a higher chlorophyll content in *Ulva prolifera*.

Wang *et al*. (2016) found higher nonphotochemical quenching coefficient in the free-floating *U. prolifera* than in the co-existing, attached *U. intestinalis* Linnaeus. Kang *et al*. (2013) made similar observations in the supralittoral *Prasiola stipitata* Suhr ex Jessen, indicating minimization of damage to the PSII complex from excess photon energy. Similarly, *M. angicava* might need to invest more energy to protect their PSII because of their parietal chloroplast position, which is more directly exposed to light than the varied chloroplast location in *P. undulatum*. The same F_V/F_M values in both *M. angicava* and *P. undulatum* indicate that the temperatures of 10 and 15°C used in the study could reflect no negative effect on PSII complexes. F_V/F_M has been widely used as a stress indicator on PSII complexes (Roháček & Barták 1999; Beer *et al*. 2014).

The physiological mechanisms underlying the difference in ϕ_{PSII} between both the species are still unknown. Further detailed investigations on light absorption and biochemical activity of PSII, and other factors affecting photosynthetic oxygen production will be necessary to understand and elucidate the underlying mechanism.

In summary, the monostromatic green benthic algae, *M. angicava* and *P. undulatum*, share similar ecological niche in the intertidal area in Muroran, Hokkaido, Japan but clearly show differences in their chloroplast localization, pigment density, absorption capacity, photosynthetic capacity, and photosynthetic efficiency. Both the species have their chloroplast along the periphery of the thallus surface, with that in *M. angicava* located uniformly on one side and the one in *P. undulatum* being surface-localized on one or the other side, or on the lateral face. The occurrence of higher chlorophyll density in *M. angicava* could explain higher photosynthesis per thallus area in them, whereas, higher efficiency of light absorption by PSII in *P. undulatum* could explain their higher photosynthesis per total chlorophyll content. These physiological differences between the two species could be an ecological strategy to balance their coexistence in the intertidal area.

ACKNOWLEDGMENTS

This study was financially supported by the Ministry of Education, Culture, Sport, Science and Technology (MEXT) through the Monbukagakusho Scholarship awarded to the first author. Appreciation is extended to the staff of Muroran Marine Station of Hokkaido University and Kobe University Research Center for Inland Seas for their valuable assistance.

REFERENCES

Arnold, K. E. and Murray, S. N. 1980. Relationship between irradiance and photosynthesis for marine benthic green algae (chlorophyta) of differing morphologies. *J. Exp. Mar. Biol. Ecol.* **43**: 183–92.

Bast, F. 2012. Systematics and taxonomic keys for the marine green algal family monostromataceae. *In* Krueger, D. and Meyer, H. (Eds). *Algae*. Nova Science Publishers, Inc., New York, pp. 105–19.

Bast, F. 2015. Taxonomic reappraisal of Monostromataceae (Ulvophyceae: Chlorophyta) based on multi-locus phylogeny. *Webbia* **70**: 43–57.

Beer, S., Björk, M. and Beardall, J. 2014. *Photosynthesis in the Marine Environment*. Wiley-Blackwell, Oxford.

Bliding, C. 1968. A critical survey of European taxa in Ulvales. Part II. *Ulva, Ulvaria, Monostroma,* Kornmannia. *Bot. Not.* **121**: 535–629.

Borlongan, I. A. G., Gerung, G. S., Nishihara, G. N. and Terada, R. 2017. Light and temperature effects on photosynthetic activity of *Eucheuma denticulatum* and *Kappaphycus alvarezii* (brown and green color morphotypes) from Sulawesi Utara, Indonesia. *Phycol. Res.* **65**: 69–79.

Britz, S. J. and Briggs, W. R. 1976. Circadian rhythms of chloroplast orientation and photosynthetic capacity in *Ulva*. *Plant Physiol.* **58**: 22–7.

Brodie, J., Maggs, C. A. and John, D. M. 2007. *The Green Seaweeds of Britain and Ireland*. British Phycological Society, Belfast.

Dawes, C. J. 1992. Irradiance acclimation of the cultured Philippine seaweeds *Kappaphycus alvarezii* and *Eucheuma denticulatum*. *Bot. Mar.* **35**: 189–95.

Frost-Christensen, H. and Sand-Jensen, K. 1992. The quantum efficiency of photosynthesis in macroalgae and submerged angiosperms. *Oecologia* **91**: 377–84.

Gayral, P. 1965. *Monostroma* Thuret, *Ulvaria* Rupr. emend. Gayral, *Ulvopsis* Gayral (Chlorophycées, Ulotrichales): structure, reproduction, cycles, position systématique. *Rev. Gén. Bot.* **72**: 627–38.

Genty, B., Briantais, J. M. and Baker, N. R. 1989. The relationship between quantum yield of photosynthetic electron transport and quenching of chlorophyll fluorescence. *Biochim. Biophys. Acta* **990**: 87–92.

Graham, L. E. and Wilcox, L. W. 2000. *Algae*. Prentice-Hall, Inc., Upper Saddle River.

Gubler, F. 1989. Immunofluorescence localisation of microtubules in plant root tips embedded in butyl-methyl methacrylate. *Cell Biol. Int. Rep.* **13**: 137–45.

Henley, W. J. 1993. Measurement and interpretation of photosynthetic light-response curves in algae in the context of photoinhibition and diel changes. *J. Phycol.* **29**: 729–39.

Hori, T. 1973. Comparative studies of pyrenoid ultrastructure in algae of the *Monostroma*-complex. *J. Phycol.* **9**: 190–9.

Ichiki, S., Mizuta, H., Yasui, H. and Yamamoto, H. 2001. Effects of irradiance and water temperature on the photosynthesis and growth of the crustose coralline alga *Lithophyllum yessoense* Foslie (Corallinales, Rhodophyceae). *Bull. Fac. Fish. Hokkaido Univ.* **52**: 103–9.

Jassby, A. D. and Platt, T. 1976. Mathematical formulation of the relationship between photosynthesis and light for phytoplankton. *Limnol. Oceanogr.* **21**: 540–7.

Kang, E. J., Scrosati, R. A. and Garbary, D. J. 2013. Physiological ecology of photosynthesis in *Prasiola stipitata* (Trebouxiophyceae) from the Bay of Fundy, Canada. *Phycol. Res.* **61**: 208–16.

Lin, A., Shen, S., Wang, G. *et al*. 2011. Comparison of chlorophyll and photosynthesis parameters of floating and attached *Ulva prolifera*. *J. Integr. Plant Biol.* **53**: 25–34.

Lobban, C. S. and Wynne, M. J. 1981. *The Biology of Seaweeds*. Blackwell Scientific Publications, Oxford.

Løvlie, A. and Bråten, T. 1970. On mitosis in the multicellular alga *Ulva mutabilis* Føyn. *J. Cell Sci.* **6**: 109–29.

Maegawa, M. and Aruga, Y. 1974. Studies on the growth and the variation of photosynthetic activity of cultivated *Monostroma latissimum*. *La mer* **12**: 27–43.

Muroran Marine Station. 2016. Sea surface water temperature in Muroran (in Japanese). [Cited on February 2017]. Available from: http://www.fsc.hokudai.ac.jp/muroran/english/kaisuion.pdf

Okazaki, K., Kabeya, Y. and Miyagishima, S. 2010. The evolution of the regulatory mechanism of chloroplast division. *Plant Signal. Behav.* **5**: 164–7.

O'Neal, S. W. and Prince, J. S. 1988. Seasonal effects of light, temperature, nutrient concentration and salinity on the physiology and growth of *Caulerpa paspaloides* (Chlorophyceae). *Mar. Biol.* **97**: 17–24.

Pellizzari, F., Oliveira, M. C., da Silva Medeiros, A., Yokoya, N. S. and Oliveira, E. C. 2013. Morphology, ontogeny, and phylogenetic position of *Gayralia brasiliensis* sp. nov. (Ulotrichales, Chlorophyta) from the southern coast of Brazil. *Bot. Mar.* **56**: 197–205.

Platt, T., Gallegos, C. L. and Harrison, W. G. 1980. Photoinhibition of photosynthesis in natural assemblages of marine phytoplankton. *J. Mar. Res.* **38**: 687–701.

Porra, R. J., Thompson, W. A. and Kriedemann, P. E. 1989. Determination of accurate extinction coefficients and simultaneous equations for assaying chlorophylls *a* and *b* extracted with four different solvents: verification of the concentration of chlorophyll standards by atomic absorption spectrometry. *Biochim. Biophys. Acta* **975**: 384–94.

Ramus, J. 1990. A form-function analysis of photon capture for seaweeds. *Hydrobiologia* **204/205**: 65–71.

Rasband, W. S. 2016. *ImageJ*. National Institutes of Health, Bethesda. [Cited on October 2016]. Available from: http://imagej.nih.gov/ij.

Roháček, K. and Barták, M. 1999. Technique of the modulated chlorophyll fluorescence: basic concepts, useful parameters, and some applications. *Photosynthetica* **37**: 339–63.

Roleda, M. Y., Hanelt, D. and Wiencke, C. 2006. Exposure to ultraviolet radiation delays photosynthetic recovery in Arctic kelp zoospores. *Photosynth. Res.* **88**: 311–22.

Shibata, K. 1959. Spectrophotometry of translucent biological materials-Opal glass transmission method. *In* Glick, D. (Ed.). *Methods of Biochemical Analysis*, *Vol.* VII. Interscience Publishers, Inc., New York, pp. 77–109.

Tatewaki, M. 1969. Culture studies on the life history of some species of the genus *Monostroma*. *Sci. Pap. Inst. Algol. Res. Fac. Sci. Hokkaido Univ.* **6**: 1–56.

Terrados, J. and Ros, J. D. 1992. The influence of temperature on seasonal variations of *Caulerpa prolifera* (Forsskal) Lamouroux photosynthesis and respiration. *J. Exp. Mar. Biol. Ecol.* **162**: 199–212.

van den Hoek, C., Mann, D. G. and Jahns, H. M. 1995. *Algae: An Introduction to Phycology*. Cambridge University Press, New York.

van Kooten, O. and Snel, J. F. H. 1990. The use of chlorophyll fluorescence nomenclature in plant stress physiology. *Photosynth. Res.* **25**: 147–50.

Vinogradova, K. L. 1969. K. istematike poryadka Ulvales (Chlorophyta) s.l. A contribution to the taxonomy of the order Ulvales. *Bot. Z.* **54**: 1347–55.

Wang, Y., Qu, T., Zhao, X., Tang, X., Xiao, H. and Tang, X. 2016. A comparative study of the photosynthetic capacity in two green tide macroalgae using chlorophyll fluorescence. *SpringerPlus* **5**: 775. Published online: 17 Jun. 2016; DOI: https://doi.org/10.1186/s40064-016-2488-7.

Watanabe, Y., Nishihara, G. N., Tokunaga, S. and Terada, R. 2014. Effect of irradiance and temperature on the photosynthesis of a cultivated red alga, *Pyropia tenera* (=*Porphyra tenera*), at the southern limit of distribution in Japan. *Phycol. Res.* **62**: 187–96.

Webb, W. L., Newton, M. and Starr, D. 1974. Carbon dioxide exchange of *Alnus rubra*: A mathematical model. *Oecologia* **17**: 281–91.

Xiao, J., Zhang, X., Gao, C. *et al*. 2016. Effect of temperature, salinity and irradiance on growth and photosynthesis of *Ulva prolifera*. *Acta Oceanol. Sin.* **35**: 114–21.

YSI Incorporated 2009. *The Dissolved Oxygen Handbook*. YSI Incorporated, Yellow Springs.

Zou, D. and Gao, K. 2014. The photosynthesis and respiratory responses to temperature and nitrogen supply in the marine green macroalga *Ulva conglobata* (Chlorophyta). *Phycologia* **53**: 86–94.

SUPPORTING INFORMATION

Additional Supporting Information may be found in the online version of this article at the publisher's web-site:

Fig. S1. A typical example of the PAM chlorophyll fluorometry in dark- and light-adapted states. F_O and F_M indicate minimum and maximum fluorescence when reaction centers in PSII are open in the dark-adapted state, respectively. F_O', F_M', and F' indicate minimum, maximum, and stable fluorescence when the reaction centers in PSII are closed in the light-adapted state, respectively. , AL, actinic light; FR, far red light; ML, measuring light, SP, saturating pulse; S, the period of measurement where the fluorescence is considered to be stable.